Fractional-statistics gas with spin and stability of the superfluid state

P. Béran
University of California, Lawrence Livermore National Laboratory, P.O. Box 808, Livermore, California 94550

R. B. Laughlin
Department of Physics, Stanford University, Stanford, California 94305
and University of California, Lawrence Livermore National Laboratory, P.O. Box 808, Livermore, California 94550
(Received 8 April 1993; revised manuscript received 25 June 1993)

The fractional-statistics gas with a spin degree of freedom is investigated using the random-phase-approximation procedure of Dai *et al.* [Phys. Rev. B **46**, 5642 (1992)]. The results are used to evaluate the stability of the superfluid state of the dilute holon system in the context of the commensurate flux phase. Spin-wave instabilities induced by gauge interactions are found to occur at extremely low density, implying that superfluidity of the fractional-statistics gas is correct in the presence of a spin degree of freedom. Spin-wave and density-wave collective excitations are also studied in presence of Coulomb repulsion between holons. The resulting instabilities at small density are estimated to occur in a density range of 0.01–0.1 holons per lattice site.

I. INTRODUCTION

The quantum mechanics of the fractional-statistics gas has been a great focus of investigation[1,2] following the suggestion[3,4] that the case of semions ($\nu=\frac{1}{2}$) may be relevant to the description of the spinless charged excitations (holons) of high-T_c superconductors. The superfluid properties of the free spinless semion gas have been demonstrated using the Hartree-Fock and random phase (RPA) approximations by Laughlin and coworkers.[5–8] Based on the commensurate flux state description of the t-J model,[9] it has been recently argued[10] that holons, in addition to fractional statistics, also exhibit a twofold degree of freedom originating from the valley degeneracy of their band structure.[11,12] This valley degeneracy is due to the magnetic structure of the translation group of holons. This degree of freedom can be thought as an "isospin." In the small doping limit, this isospin becomes a good quantum number and the holon system can be described as an unpolarized system of semions with isospin, in which both isospin states are equally occupied.

Zou, Levy, and Laughlin[10] pointed out that the physical behavior of the semion gas may be changed by the presence of this isospin degree of freedom. In the Hartree-Fock treatment, this difficulty is associated with the fact that the relative angular momentum of a pair of semions is quantized by fractional statistics and leads to an arbitrarily large kinetic energy when the particles come close to each other. This does not affect particles with identical isospin, which are constrained by the structure of the Hartree-Fock ground state to stay well apart from each other. However, particles with opposite isospin are not subject to this correlation and may reach the closest approach which, in the case of holons, is given by the lattice spacing. Thus, the contributions to kinetic energy originating from the relative angular momentum of particles with opposite isospin are characterized by the length scale of the lattice spacing while those originating from the relative angular momentum of particles with identical isospin are characterized by the mean interholon distance. In the small doping limit, the former contributions are expected to dominate and to destabilize the Hartree-Fock ground state, which provides the basis for discussing the superfluid properties of the semion system.

It is legitimate to address the question of the strength of this isospin-induced instability at small doping and to ask if this instability can invalidate predictions of superfluidity at holon densities relevant to the experimental observation of high-temperature superconductivity. In this paper, we study this instability at zero temperature using the Hartree-Fock and RPA procedures[8] for a simple model of free semions with an isospin in the continuous space. In this model, the finite lattice spacing of the real system is simulated by a short-range cutoff of the fractional statistics interaction. We find the instability of the isospin-unpolarized system to occur at a density smaller than 2×10^{-5} holons per lattice site, well below the doping range 0.15–0.2 of interest for the experiment.[13] This instability is characterized by the softening of a collective mode of the unpolarized system which is identified as an isospin density fluctuation.[14] This softening can be regarded as an indication of "isospin antiferromagnetic" long-range order, leading to destruction of superfluidity. The low value of the critical density is due to the logarithmic dependence of the roton minimum associated with the isospin density wave as a function of the holon density. Because of the logarithmic dependence of its strength, this instability only weakly affects the speed of sound of the superfluid in the density range of interest for the experiment. This leads to the conclusion that the isospin-induced instability has no physical relevance in the case of free semions.

We also study these instabilities of the semion system

0163-1829/93/48(14)/10382(9)/$06.00

at small density in the presence of the Coulomb repulsion between charged holons. We first study the instability toward Wigner crystallization of the isospin-polarized semion system and of the spinless boson system and find this instability to occur at a significantly higher density for semions than for bosons. We then study the instability of the unpolarized semion system and find this instability to be of isospin-wave type and to occur at a relatively large density. Based on these results, we roughly estimate the critical density of the superfluid holon system to lay in the range of 10^{-1}–10^{-2} holons per lattice site and speculate on the relevance of this instability to the disappearance of high-temperature superconductivity at small doping.

II. FRACTIONAL-STATISTICS HAMILTONIAN

Let us begin the discussion by restating the problem of free semions with an isospin in the Fermi representation. Following Ref. 8, we represent the ideal fractional statistics gas by a system of fermions with an isospin described by the Hamiltonian

$$\mathcal{H}=\frac{1}{2}\sum_{i=1}^{N}|\mathbf{P}_i+\mathbf{A}_i|^2 , \tag{1}$$

where $\nu=\frac{1}{2}$ for semions and where

$$\mathbf{A}_i=\sum_{j\neq i}^{N}\mathbf{A}_{ij}=\frac{1}{2}\sum_{j\neq i}^{N}\hat{\mathbf{z}}\times\frac{\mathbf{r}_i-\mathbf{r}_j}{|\mathbf{r}_i-\mathbf{r}_j|^2} . \tag{2}$$

In this system each fermion i interacts with all the others through vector potentials $\mathbf{A}_{ij}$ for $j\neq i$, which are generated by solenoids attached to the fermions. In writing Eqs. (1) and (2), we have used dimensionless units in which the effective cyclotron energy[8]

$$\hbar\omega_c=\frac{\pi\hbar^2}{m^*}\bar{\rho} \tag{3}$$

and the corresponding magnetic length

$$a_0=\left[\frac{\hbar}{m^*\omega_c}\right]^{1/2}=\frac{1}{\sqrt{\pi\bar{\rho}}} \tag{4}$$

are set to unity. Here, $\bar{\rho}$ and m^* denote the holon density and the effective mass, respectively.

The problem associated with the isospin is first manifested by the divergence of the Hartree-Fock energy of the unpolarized state.[10] This divergence is due to the term $|\mathbf{A}_{ij}|^2$ appearing in the Hamiltonian $\mathcal{H}$, which can be regarded as a short-range repulsion. This repulsion affects particles i and j with identical spin minimally, because the Hartree-Fock wave function vanishes at particle coincidence. However, within the Hartree-Fock approximation particles with opposite spin are not correlated and can come arbitrarily close to each other, leading to an infinite contribution for the mean-field interaction energy $|\mathbf{A}_{ij}|^2$.

Clearly, this divergence at short interparticle distance is an artifact of the model of semions in the continuous space. Indeed, it cannot apply to the case of interest given by the commensurate flux state,[10] in which holons are confined on a lattice and in which no site can be doubly occupied, leading to a minimal interholon distance given by the lattice spacing. The failure of the continuous model is due to the fact that it does not take into account the uncertainty in the position of the holon which results from its confinement into a given degenerate valley[12,10] in momentum space, or in other words, from the definition of the isospin. This uncertainty is of the order of the lattice spacing. If we insist on treating the holon system as an ideal gas of semions in the continuous space, this uncertainty in the holon position may be taken into account by introducing an effective cutoff in the vector potential $\mathbf{A}_{ij}$ at an interholon distance $|\mathbf{r}_i-\mathbf{r}_j|$ smaller than the lattice spacing. We shall do this using a Hamiltonian of the form

$$\tilde{\mathcal{H}}=\frac{1}{2}\sum_{i=1}^{N}|\mathbf{P}_i+\tilde{\mathbf{A}}_i|^2 , \tag{5}$$

where

$$\tilde{\mathbf{A}}_i=\sum_{j\neq i}^{N}\tilde{\mathbf{A}}_{ij}=\frac{1}{2}\sum_{j\neq i}^{N}\hat{\mathbf{z}}\times\frac{\mathbf{r}_i-\mathbf{r}_j}{|\mathbf{r}_i-\mathbf{r}_j|^2}(1-e^{-\alpha|z_i-z_j|^2/2}) , \tag{6}$$

and α is a parameter. This substitution effectively gives a finite size to the flux tubes attached to each fermion. It is appropriate for studying the isospin-induced instability but not for obtaining accurate results for the system of semions on the lattice.

The instability associated with the isospin results from the dominance of the "potential" energy $\tilde{A}_{ij}^2$ in the limit $\alpha\to\infty$ of dilute systems, where the cutoff range becomes vanishingly small. This is reminiscent of the Coulomb gas of electrons which, at small density, tends to minimize its potential energy to the detriment of kinetic energy, leading to instabilities toward full spin-polarization and Wigner crystallization.[15,16]

The cutoff at short interparticle distance can also be introduced by using the effective Hamiltonian

$$\tilde{\mathcal{H}}_{\text{eff}}=\lim_{\alpha\to\infty}\left[\frac{1}{2}\sum_{i=1}^{N}|\mathbf{P}_i+\tilde{\mathbf{A}}_i|^2-\frac{\pi}{8}\ln\left[\frac{\alpha}{\alpha'}\right]\sum_{j\neq i}\delta(\mathbf{r}_i-\mathbf{r}_j)\right] , \tag{7}$$

where $\tilde{\mathbf{A}}_i$ is given by Eq. (6) as a function of α and where α' is now the parameter reflecting the holon doping. In this Hamiltonian, the divergent contribution to the Hartree-Fock energy due to the interaction $|\mathbf{A}_{ij}|^2$ between particles with opposite isospin is canceled by an attractive delta-function potential. This effective Hamiltonian leads to simple analytical results and is repeatedly used in our study of the isospin-induced instability.

III. POLARIZED VERSUS UNPOLARIZED STATE

Keeping in mind its analogy with the Coulomb gas, we first study the instability of the semion system toward full polarization by comparing the expectation energy of the polarized and unpolarized Hartree-Fock ground states.

Both states are constructed using a Slater determinant of the form

$$\Phi(\mathbf{r}_1,\sigma_1,\ldots,\mathbf{r}_N,\sigma_N) = \frac{1}{\sqrt{N!}}\sum_{P}^{N!}(-1)^{[P]}\phi_1(\mathbf{r}_{P_1},\sigma_{P_1})\cdots\phi_N(\mathbf{r}_{P_N},\sigma_{P_N}) , \tag{8}$$

where $\sigma_i=\uparrow,\downarrow$ denotes the isospin of particle i and where the single-particle wave functions $\phi_i(\mathbf{r},\sigma)$ are given by

$$\phi_i(\mathbf{r},\sigma)=\begin{cases}\phi^{\uparrow}_{0,i}(\mathbf{r},\sigma), & i=1,\ldots,N/2\\ \phi^{\uparrow}_{1,i-N/2}(\mathbf{r},\sigma), & i=1+N/2,\ldots,N\end{cases} \tag{9}$$

in the case of the polarized state and by

$$\phi_i(\mathbf{r},\sigma)=\begin{cases}\phi^{\uparrow}_{0,i}(\mathbf{r},\sigma), & i=1,\ldots,N/2\\ \phi^{\downarrow}_{0,i-N/2}(\mathbf{r},\sigma), & i=1+N/2,\ldots,N\end{cases} \tag{10}$$

in the case of the unpolarized state, where

$$\phi^{\sigma'}_{n,k}(\mathbf{r},\sigma)=\delta_{\sigma'\sigma}\frac{(a^{\dagger})^n}{\sqrt{2^n n!}}\frac{(b^{\dagger})^k}{\sqrt{2^k k!}}\frac{e^{-|z|^2/4}}{\sqrt{2\pi}} \tag{11}$$

are orbitals with isospin polarization $\sigma'=\uparrow,\downarrow$ expressed as a function of the Landau level- and angular momentum-raising operators

$$a^{\dagger}=\frac{z}{2}-2\frac{\partial}{\partial_{z^*}} \tag{12}$$

and

$$b^{\dagger}=\frac{z^*}{2}-2\frac{\partial}{\partial_z} , \tag{13}$$

and where $z=x+iy$.

Using the Hamiltonian of Eq. (5), we evaluate the expectation energy

$$\langle\tilde{\mathcal{H}}\rangle=\frac{\langle\Phi|\tilde{\mathcal{H}}|\Phi\rangle}{\langle\Phi|\Phi\rangle} \tag{14}$$

by following the procedure of Ref. 5. We respectively obtain for the polarized and unpolarized states

$$\frac{\langle\tilde{\mathcal{H}}\rangle_{\uparrow\uparrow}}{N}=\frac{27}{32}+\frac{2\alpha^6+8\alpha^5+17\alpha^4+18\alpha^3+11\alpha^2+4\alpha+1}{16(\alpha+1)^6}-\frac{\alpha^2}{16(\alpha+2)^2}+\frac{8\alpha+3}{32(2\alpha+1)^2}+\frac{1}{8}\ln\left[\frac{(2\alpha+1)(\alpha+2)}{2(\alpha+1)^2}\right] , \tag{15}$$

and

$$\frac{\langle\tilde{\mathcal{H}}\rangle_{\uparrow\downarrow}}{N}=\frac{1}{2}-\frac{\alpha(3\alpha+4)}{16(\alpha+1)^2}+\frac{1}{16}\ln\left[\frac{(\alpha+2)^2(2\alpha+1)}{(2\alpha+2)^2}\right] . \tag{16}$$

Note the logarithmic divergence at large values of α of the Hartree-Fock energy of the unpolarized state. Now, using the effective Hamiltonian $\tilde{\mathcal{H}}_{\text{eff}}$ of Eq. (7) instead of $\tilde{\mathcal{H}}$, we find

$$\frac{\langle\tilde{\mathcal{H}}_{\text{eff}}\rangle_{\uparrow\uparrow}}{N}=\frac{29}{32} \tag{17}$$

and

$$\frac{\langle\tilde{\mathcal{H}}_{\text{eff}}\rangle_{\uparrow\downarrow}}{N}=\frac{1}{16}[5+\ln(\alpha'/2)] . \tag{18}$$

These energies are equivalent to those of Eqs. (15) and (16) when $\alpha'=\alpha$ and when $\alpha\to\infty$ and essentially lead to identical results for the critical density at which the expected energies of polarized and unpolarized states cross over. We find $\alpha'_{\text{crossover}}=2e^{19/2}$. Let us now take α' to be

$$\alpha'=1/\pi\delta , \tag{19}$$

where δ is the average number of holons per site. This is equivalent to taking $\alpha'=(a_0/b_0)^2$, where a_0 is given by Eq. (4) and b_0 is the lattice spacing. We then find that the crossover occurs at a doping of $\delta=1.2\times10^{-5}$. We conclude from this that this isospin polarization is irrelevant in the doping range of interest ($\delta\cong0.1$).

The speed of sound of the superfluid can be estimated[5] from the compressibility corresponding to the energy of the unpolarized state. The compressibility and the speed of sound v_s diverge very slowly in the limit of the dilute system as a consequence of the logarithmic divergence of the energy. For example, at densities corresponding to 0.3 and 0.03 holons per lattice site we respectively obtain $v_s=0.92$ and 0.94 in units of $\omega_c a_0$.

It is known from the study[15,16] of the electron gas that the introduction of correlation between particles with opposite spin significantly reduces the energy of the unpolarized state and thus lowers the critical density at which spin polarization occurs. Since this correlation is not taken into account in the present work, our result should be regarded as an upper bound for the critical density of the instability toward isospin polarization.

IV. COLLECTIVE MODE SPECTRUM

A. RPA procedure

In this section, we study the collective modes of the unpolarized semion system using the RPA procedure of Ref. 8. We first present the RPA treatment of the semion system in the presence of a spin degree of freedom $s=\frac{1}{2}$. We then introduce a short-range cutoff in the vector potential in order to remove the divergence associated with the spin.

The analysis of collective modes of the semion gas involves the evaluation of the four-point Green's function

$$\mathcal{F}(\mathbf{r}_1\sigma_1,\mathbf{r}_4\sigma_4|\mathbf{r}_2\sigma_2,\mathbf{r}_3\sigma_3)=\frac{i}{\hbar}\int_{-\infty}^{\infty}dt\, e^{-i\omega t}\langle 0|T[\hat{\psi}_{\sigma_1}(\mathbf{r}_1,t)\hat{\psi}^{\dagger}_{\sigma_4}(\mathbf{r}_4,t)\hat{\psi}^{\dagger}_{\sigma_2}(\mathbf{r}_2,0)\hat{\psi}_{\sigma_3}(\mathbf{r}_3,0)]|0\rangle \tag{20}$$

describing the propagation of a particle-hole pair, where $\sigma=\uparrow,\downarrow$ denotes the spin variable and where

$$\hat{\psi}_\sigma(\mathbf{r},t)=e^{(i/\hbar)\mathcal{H}t}\psi_\sigma(\mathbf{r})e^{-(i/\hbar)\mathcal{H}t} \tag{21}$$

is the Heisenberg version of the operator $\psi_\sigma(\mathbf{r})$.

Due to the fact that the total spin is conserved, Eq. (20) can be diagonalized in its spin variables to yield the singlet or triplet Green's function

$$\mathcal{F}^{\text{singlet}}(\mathbf{r}_1\mathbf{r}_4|\mathbf{r}_2\mathbf{r}_3)=\sum_{\sigma_1\cdots\sigma_4}\frac{1}{2}\delta_{\sigma_1\sigma_4}\delta_{\sigma_2\sigma_3}\times\mathcal{F}(\mathbf{r}_1\sigma_1,\mathbf{r}_4\sigma_4|\mathbf{r}_2\sigma_2,\mathbf{r}_3\sigma_3) \tag{22}$$

or

$$\mathcal{F}^{\text{triplet}}(\mathbf{r}_1\mathbf{r}_4|\mathbf{r}_2\mathbf{r}_3)=\sum_{\sigma_1\cdots\sigma_4}\frac{1}{3}\left[\delta_{\sigma_1\sigma_2}\delta_{\sigma_3\sigma_4}-\frac{1}{2}\delta_{\sigma_1\sigma_4}\delta_{\sigma_2\sigma_3}\right]\times\mathcal{F}(\mathbf{r}_1\sigma_1,\mathbf{r}_4\sigma_4|\mathbf{r}_2\sigma_2,\mathbf{r}_3\sigma_3) \tag{23}$$

describing the propagation of a particle-hole pair in a singlet state with fixed total spin $S=0$ or in a triplet state with fixed total spin $S=1$.

It is convenient[8] to express these four-point Green's functions in terms of their matrix elements

$$\langle {}^{m'}_{m}|\mathcal{F}|^{n'}_{n}\rangle=\int d^2r_1d^2r_2d^2r_3d^2r_4\psi^{m'*}_{m\alpha}(\mathbf{r}_1,\mathbf{r}_4)\times\mathcal{F}(\mathbf{r}_1,\mathbf{r}_4|\mathbf{r}_2,\mathbf{r}_3)\psi^{n'}_{n\beta}(\mathbf{r}_2,\mathbf{r}_3) \tag{24}$$

on the basis of magnetoexciton wave functions

$$\psi^{n'}_{n\beta}(\mathbf{r}_1,\mathbf{r}_2)=\frac{(-1)^n}{L\sqrt{2\pi 2^{n+n'}n!n'!}}(2\partial_{z_1^*}-z_1/2)^n(2\partial_{z_2}-z_2^*/2)^{n'}\exp[-\tfrac{1}{4}(|z_1|^2+|z_2|^2+|z_\beta|^2)]\exp[\tfrac{1}{2}(z_1^*z_2+z_1^*z_\beta-z_2z_\beta^*)] , \tag{25}$$

where z_β is given by $z_\beta=i(q_x+iq_y)$ as a function of the momentum $\mathbf{q}$ of the particle-hole pair. The momentum $\mathbf{q}$ is conserved.[8] The singlet and triplet collective mode spectra are evaluated for given momentum $\mathbf{q}$ as the set of values for frequency ω leading to a singular matrix (24) for the four-point Green's function, i.e.,

$$\det\left[\mathcal{F}^{\text{singlet}}\right]^{-1}=0 ,\qquad \det\left[\mathcal{F}^{\text{triplet}}\right]^{-1}=0 . \tag{26}$$

The collective modes for $S=0$ correspond to density waves in which density oscillations occur in phase for both spin species while those for $S=1$ correspond to spin waves in which the density of particles with spin up and the density of particles with spin down oscillate in opposite phase.

The four-point Green's function of the unpolarized semion system can be evaluated as a sum of Hartree, exchange, ladder, and RPA graphs using the procedure of Ref. 8. Using length and energy units of Eqs. (3) and (4), we obtain

$$\left[\mathcal{F}^{\text{singlet}}\right]^{-1}\cong(\mathcal{F}_0)^{-1}-\sum_{i=1}^{20}a_i^{\text{singlet}}\mathcal{W}^{(i)} \tag{27}$$

and

$$\left[\mathcal{F}^{\text{triplet}}\right]^{-1}\cong(\mathcal{F}_0)^{-1}-\sum_{i=1}^{20}a_i^{\text{triplet}}\mathcal{W}^{(i)} , \tag{28}$$

where $\mathcal{F}_0$ is given by

$$\langle {}^{m'}_{m}|\mathcal{F}_0|^{n'}_{n}\rangle=\delta_{\alpha\beta}\delta_{mn}\delta_{m'n'}\begin{cases}[\hbar\omega-(\epsilon_n-\epsilon_{n'})+i\eta]^{-1}, & n'=0,n>0\\ [-\hbar\omega-(\epsilon_{n'}-\epsilon_n)+i\eta]^{-1}, & n=0,n'>0\\ 0, \text{ otherwise} ,\end{cases} \tag{29}$$

where

$$\epsilon_n=\sum_{i=1}^{12}b_i\epsilon_n^{(i)} . \tag{30}$$

The coefficients a_i and b_i are listed in Tables I and II. The quantities $\epsilon_n^{(i)}$ and $\mathcal{W}^{(i)}$ are defined by Eqs. (3.4)–(3.15) of Ref. 5 and Eqs. (7.9)–(7.28) of Ref. 8, and are given explicitly in Appendixes A, D, and E of Ref. 8. Typical examples are

$$\epsilon_n^{(5)}=-\tfrac{1}{4} , \tag{31}$$

which corresponds to Eq. (A4) of Ref. 5 and

$$\langle {}^{0}_{m}|\mathcal{W}^{(8)}|^{0}_{n}\rangle=\delta_{\alpha\beta}\frac{(-z_\beta^*)^m(-z_\beta)^n}{\sqrt{2^{m+n+4}m!n!}}\times e^{-|z_\beta|^2/2}(2m/|z_\beta|^2-1) , \tag{32}$$

which corresponds to Eq. (D8) of Ref. 8.

Note that Appendixes A, D, and E of Ref. 8, where these quantities are listed, refer to a gas of *bosons* ($\nu=0$) rather than a gas of semions. This is because the in-

TABLE I. Coefficients a_i multiplying quantities $\mathcal{W}^{(i)}$, as defined by Eqs. (27) and (28).

i	a_i^{singlet}	a_i^{triplet}	i	a_i^{singlet}	a_i^{triplet}
1	1	0	11	$\frac{1}{2}$	0
2	1	0	12	$\frac{1}{2}$	0
3	$\frac{1}{2}$	$\frac{1}{2}$	13	$\frac{1}{2}$	0
4	$\frac{1}{2}$	$\frac{1}{2}$	14	1	0
5	$\frac{1}{2}$	0	15	$\frac{1}{4}$	$\frac{1}{4}$
6	$\frac{1}{4}$	$\frac{1}{4}$	16	$\frac{1}{4}$	$\frac{1}{4}$
7	$\frac{1}{2}$	$\frac{1}{2}$	17	$\frac{1}{4}$	$\frac{1}{4}$
8	$\frac{1}{2}$	0	18	$\frac{1}{4}$	$\frac{1}{4}$
9	$\frac{1}{2}$	0	19	$\frac{1}{4}$	$\frac{1}{4}$
10	$\frac{1}{2}$	0	20	$\frac{1}{4}$	$\frac{1}{4}$

tegrals for the semion gas with isospin are the same as those for the bose gas, except for a change in the length and energy units and the spin multiplicity factor. These effects are accounted for by the factors a_i and b_i in Tables I and II. The singlet and triplet coefficients are different because the RPA graphs are zero for the triplet, due to spin conservation at the vertex. The coefficient a_i or b_i is essentially the spin multiplicity of the corresponding graph, evaluated with the usual Feynman rules, times a factor $\frac{1}{2}$ for each occurrence of A_{ij} in the relevant integral.

As in the Hartree-Fock calculation, we now encounter a short-wavelength divergence associated with the spin degree of freedom. The formally divergent integral

$$I_2 = e^{-q^2/2} \lim_{\eta\to 0} \int_0^\infty r\,dr\, \frac{e^{-r^2/2}}{r^2+\eta^2}\ , \tag{33}$$

which appears with opposite signs in the ladder diagram $\mathcal{W}^{(6)}$ and in the sum of RPA diagrams $\mathcal{W}^{(5)}+\mathcal{W}^{(12)}+\mathcal{W}^{(13)}$, no longer cancels as it did in the case of spinless semions.[8] Like for the isospin polarization discussed in Sec. III, this divergence is an artifact of the continuum that may be rectified by substituting the effective Hamiltonian $\tilde{\mathcal{H}}_{\text{eff}}$ of Eq. (7) for $\mathcal{H}$. This modifies I_2 to

$$I_2 \to \frac{e^{-q^2/2}}{2} \ln\left[\frac{\alpha'}{2}\right] \tag{34}$$

and has no other effect.

TABLE II. Coefficients b_i multiplying quantities $\epsilon_n^{(i)}$, as defined by Eq. (30).

i	b_i	i	b_i
1	1	7	$\frac{1}{4}$
2	1	8	$\frac{1}{4}$
3	$\frac{1}{2}$	9	$\frac{1}{4}$
4	$\frac{1}{2}$	10	$\frac{1}{4}$
5	$\frac{1}{2}$	11	$\frac{1}{2}$
6	$\frac{1}{2}$	12	$\frac{1}{2}$

B. Results

In Fig. 1, we show the dispersion relation of the collective modes associated with the triplet (dashed lines) and with the singlet (full lines) for values of the parameter $\alpha'=1$, 3×10^2, and 1.65×10^4, which respectively correspond to 0.32, 1×10^{-3}, and 1.9×10^{-5} holons per lattice site. The softening of the roton in the triplet channel for the last value of parameter α' corresponds to an instability toward an isospin density wave. Note that the wavelength $\lambda=2\pi/q$ associated with the roton minimum is twice the mean interparticle distance.

The density at which this "antiferromagnetic" instability occurs is nearly identical to the critical density found in Sec. III for the "ferromagnetic" instability. Thus, the two calculations corroborate each other. It often occurs in interacting Fermi systems, which are similar, that competing instabilities become important at roughly the same density.[17] While the phase diagram is difficult to calculate reliably near this density, the existence of an instability of some kind is clear. As remarked in Sec. III, it is important for the anyon description of high-temperature superconductivity that this density is low.

The energy of the triplet collective mode remains finite at large wavelength, as occurs with the collective mode energy of quantum Hall states.[18] This is due to the fact that the RPA diagrams, which have been found[6] to be responsible for the linear dispersion relation of compressional sound in this system at large wavelength, are absent in the triplet channel. It is interesting to note the absence of a roton in the singlet channel at any density. This is similar to the well-known behavior of Fermi systems with short-range repulsions, in which the instability toward antiferromagnetism is much stronger than the instability toward Wigner crystallization.[19]

V. SPIRAL SPIN DENSITY WAVE

We present here the relation between the collective mode obtained within the RPA procedure and the description[14,20] of a spiral spin density wave. This allows us to put our work in perspective with previous stud-

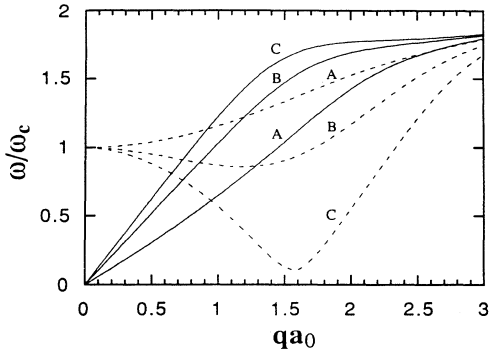

FIG. 1. Dispersion relations of the triplet (dashed lines) and singlet (full lines) collective modes of the isospin-unpolarized semion system for values of the parameter (A) $\alpha'=1$, (B) $\alpha'=3\times10^2$, and (C) $\alpha'=1.65\times10^4$.

ies[14,20–22] concerning the antiferromagnetic instability of the Fermi gas.

Let us consider a Slater determinant of the form of Eq. (8) constructed using the orbitals

$$\phi_i(\mathbf{r},\sigma)=\begin{cases}\phi^{\uparrow}_{0,i}(\mathbf{r},\sigma)+e^{\frac{(z_\beta b^\dagger - z^*_\beta b)}{2}}\sum_{n=1}^{\infty}\frac{c_n^0(a^\dagger)^n}{\sqrt{2^n n!}}\phi^{\downarrow}_{0,i}(\mathbf{r},\sigma), & i=1,\ldots,N/2\\ \phi^{\downarrow}_{0,i-N/2}(\mathbf{r},\sigma)+e^{\frac{(z^*_\beta b - z_\beta b^\dagger)}{2}}\sum_{n=1}^{\infty}\frac{(-1)^n(c_0^n)^*(a^\dagger)^n}{\sqrt{2^n n!}}\phi^{\uparrow}_{0,i-N/2}(\mathbf{r},\sigma), & i=1+N/2,\ldots,N\end{cases} \tag{35}$$

where the operators $a^\dagger$ and $b^\dagger$ are defined as in Eqs. (12) and (13), $z_\beta = i(q_x + iq_y)$, and where the c's are variational parameters.

This state is a spin density wave of momentum $\mathbf{q}$ in which the spin spirals in the plane perpendicular to its axis of quantization, as indicated by the expectation value of the spin at given position $\mathbf{r}$. This expectation value is given by

$$\langle \psi^\dagger_{\sigma_1}(\mathbf{r})\psi_{\sigma_2}(\mathbf{r})\rangle_{SW}=\frac{1}{2\pi}\left[\delta_{\sigma_1\sigma_2}+\delta_{\sigma_1\downarrow}\delta_{\sigma_2\uparrow}Ae^{(z^*z_\beta - zz^*_\beta)/2}+\delta_{\sigma_1\uparrow}\delta_{\sigma_2\downarrow}A^*e^{-(z^*z_\beta - zz^*_\beta)/2}\right]+O^2(c_n^{n'}) , \tag{36}$$

where $z = x + iy$ and

$$A = e^{-|z_\beta|^2/4}\sum_{n=1}^{\infty}(-1)^n\frac{c_n^0 z_\beta^n + c_0^n z_\beta^{*n}}{\sqrt{2^n n!}} . \tag{37}$$

This state is formally similar to the wave function describing the spin density-wave instability of the Coulomb gas.[14] It may be viewed as a coherent superposition of triplet particle-hole pairs excited out of the Hartree-Fock vacuum described by Eqs. (8) and (10).

The relation between this wave function and the perturbative calculation of previous section can be established by evaluating its expectation energy $\langle \tilde{\mathcal{H}}_{\rm eff}\rangle_{SW}$ using the effective Hamiltonian of Eq. (7). Expanding this expectation energy in powers of c_n^0 and c_0^n and retaining only linear and quadratic terms, we find

$$\frac{\langle \tilde{\mathcal{H}}_{\rm eff}\rangle_{SW}-\langle \tilde{\mathcal{H}}_{\rm eff}\rangle_{\uparrow\downarrow}}{N} = -\frac{1}{2}\sum_{mm'nn'}(c_m^{m'})^*\langle {}^{m'}_{m}|(\mathcal{F}^{\rm triplet})^{-1}|^{n'}_{n}\rangle|_{\omega=0} \times c_n^{n'}+O^3(c_n^{n'}) , \tag{38}$$

where $\mathcal{F}^{\rm triplet}$ is defined as in Eq. (28). Thus $\mathcal{F}^{\rm triplet}$ corresponds exactly to a linear response kernel in the c's. It follows that the eigenvector of $\mathcal{F}^{\rm triplet}$ that becomes singular at the instability point corresponds to a specific wave function of this form.

VI. COULOMB INTERACTION

A. RPA procedure

In units of the effective cyclotron energy $\hbar\omega_c$ and of the effective magnetic length a_0, the Hamiltonian appropriate for a system of particles with charge e obeying fractional statistics is given by

$$\mathcal{H}_{\rm tot}=\mathcal{H}+\frac{r_s}{2}\sum_{i\neq j}\frac{1}{|\mathbf{r}_i-\mathbf{r}_j|}-r_s\bar{\rho}\sum_j\int_{\rm sample}\frac{d^2r}{|\mathbf{r}-\mathbf{r}_j|} , \tag{39}$$

where $\mathcal{H}$ is defined as in Eq. (1) and where r_s is a dimensionless parameter reflecting the mean inter-particle distance. The latter is given by

$$r_s=\frac{m^*e^2}{\varepsilon\hbar^2}\frac{1}{\sqrt{\pi\bar{\rho}}} , \tag{40}$$

where ε is the dielectric constant of the medium and where m^* is the effective mass of the holon.

We first consider the isospin-unpolarized semion system. In the presence of Coulomb interactions, the four-point Green's function $\mathcal{F}$ is now given by

$$(\mathcal{F}^{\rm singlet})^{-1}\cong(\mathcal{F}_0)^{-1}-\sum_{i=1}^{22}a_i^{\rm singlet}\mathcal{W}^{(i)} \tag{41}$$

and

$$(\mathcal{F}^{\rm triplet})^{-1}\cong(\mathcal{F}_0)^{-1}-\sum_{i=1}^{22}a_i^{\rm triplet}\mathcal{W}^{(i)} , \tag{42}$$

where coefficients a_{21} and a_{22} are listed in Table III and where $\mathcal{F}_0$ is given by Eq. (29) with

$$\epsilon_n=\sum_{i=1}^{13}b_i\epsilon_n^{(i)} , \tag{43}$$

where $b_{13}=1$. The additional diagrams $\epsilon^{(13)}$, $\mathcal{W}^{(21)}$, and $\mathcal{W}^{(22)}$ appearing in Eqs. (41)–(43) are

$$\begin{aligned}\epsilon_n^{(13)}&=-\frac{2\pi}{L^2}\int d^2r_1d^2r_2\frac{r_s}{|\mathbf{r}_1-\mathbf{r}_2|}\Pi_n(\mathbf{r}_1,\mathbf{r}_2)\Pi_0(\mathbf{r}_2,\mathbf{r}_1) ,\\ \langle {}^{m'}_{m}|\mathcal{W}^{(21)}|^{n'}_{n}\rangle&=\int d^2r_1d^2r_2\frac{r_s}{|\mathbf{r}_1-\mathbf{r}_2|}\psi^{m'*}_{m\alpha}(\mathbf{r}_1,\mathbf{r}_1)\times\psi^{n'}_{n\beta}(\mathbf{r}_2,\mathbf{r}_2) ,\\ \langle {}^{m'}_{m}|\mathcal{W}^{(22)}|^{n'}_{n}\rangle&=-\int d^2r_1d^2r_2\frac{r_s}{|\mathbf{r}_1-\mathbf{r}_2|}\psi^{m'*}_{m\alpha}(\mathbf{r}_1,\mathbf{r}_2)\times\psi^{n'}_{n\beta}(\mathbf{r}_1,\mathbf{r}_2) ,\end{aligned} \tag{44}$$

where Π_n is the projector[5] onto the nth Landau level

given by

$$\Pi_n(\mathbf{r}_1,\mathbf{r}_2)=\frac{1}{2\pi}L_n\left[\frac{|z_1-z_2|^2}{2}\right]\times\exp[-\tfrac{1}{4}(|z_1|^2+|z_2|^2)+\tfrac{1}{2}z_1^*z_2] \quad (45)$$

and where L_n is the nth Laguerre polynomial. Explicit expressions for these quantities are listed in the Appendix. In order to introduce a cutoff at short interparticle distance, we replace the bare Hamiltonian $\mathcal{H}$ in Eq. (39) by the effective Hamiltonian $\tilde{\mathcal{H}}_{\rm eff}$ of Eq. (7) with $\alpha'=2$.

We then consider the isospin-polarized semion system.

TABLE III. Coefficients a_i multiplying quantities $\mathcal{W}^{(i)}$, as defined by Eqs. (41) and (42).

i	$a_i^{\rm singlet}$	$a_i^{\rm triplet}$	i	$a_i^{\rm singlet}$	$a_i^{\rm triplet}$
21	2	0	22	2	0

For this we have

$$(\mathcal{J})^{-1}\cong(\mathcal{J}_0)^{-1}-\sum_{i=1}^{22}\mathcal{W}^{(i)} \quad (46)$$

with

$$\langle {}^{m'}_{m}|\mathcal{J}_0|{}^{n'}_{n}\rangle=\delta_{\alpha\beta}\delta_{mn}\delta_{m'n'}\begin{cases}[\hbar\omega-(\epsilon_n-\epsilon_{n'})+i\eta]^{-1}, & n'=0,\ 1,\ n>1\\ [-\hbar\omega-(\epsilon_{n'}-\epsilon_n)+i\eta]^{-1}, & n=0,\ 1,\ n'>1\\ 0, \quad \text{otherwise}\ ,\end{cases} \quad (47)$$

where

$$\epsilon_n=\sum_{i=1}^{13}\epsilon_n^{(i)}\ . \quad (48)$$

Please note that the quantities $\epsilon_n^{(1)}\cdots\epsilon_n^{(12)}$ and $\mathcal{W}^{(1)}\cdots\mathcal{W}^{(20)}$ of Eqs. (47) and (48) refer now to an unperturbed polarized ground state with Landau levels $n=0$ and 1 occupied. These quantities are now given by Appendixes B, F, and G of Ref. 8.

B. Results

Let us first consider the magnetic instabilities of semions with an isospin. Following Eqs. (17) and (18), we have for the energies of the polarized and unpolarized states in the presence of Coulomb repulsion

$$\frac{\langle\tilde{\mathcal{H}}_{\rm eff}\rangle_{\uparrow\uparrow}}{N}=\frac{29}{32}-\frac{11}{16}\left[\frac{\pi}{2}\right]^{1/2}r_s \quad (49)$$

and

$$\frac{\langle\tilde{\mathcal{H}}_{\rm eff}\rangle_{\uparrow\downarrow}}{N}=\frac{1}{16}[5+\ln(\alpha'/2)]-\frac{1}{2}\left[\frac{\pi}{2}\right]^{1/2}r_s\ . \quad (50)$$

Taking $\alpha'=2$ as discussed in the previous section, we find the critical r_s at which the expected energies of the polarized and unpolarized states cross over to be $r_s^{\rm crossover}=(\frac{19}{6})\sqrt{2/\pi}$, or 2.53.

Now, in Fig. 2 we show the dispersion relations of the collective modes associated with the triplet (dashed) and singlet (solid) channels of the isospin-unpolarized system of semions with Coulomb interaction. Note the similarity with Fig. 1. The softening of the triplet mode at $r_s=2.36$ corresponds to the onset of antiferromagnetic long-range order. The singlet mode disperses like the square root of q at large wavelength, as appropriate for the two-dimensional plasmon.[23] Again, we see no significant roton formation in the singlet channel. This is due to the fact that, in absence of correlation between particles with opposite isospin in the unperturbed Hartree-Fock ground state, the short-range part of the Coulomb repulsion favors spin-wave instabilities to the detriment of density-wave instabilities.[19]

We now consider the instabilities toward Wigner crystallization of the isospin-polarized semion system. In Fig. 3, we show the collective mode frequency for this system in presence of Coulomb repulsion. The softening of the collective mode at $r_s=9.95$ corresponds to Wigner crystallization. Note that the wavelength associated with the roton minimum now equals the mean interparticle distance, as opposed to twice this distance, as occurs in Figs. 1 and 2.

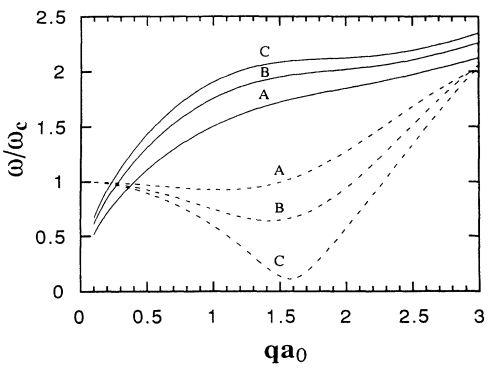

FIG. 2. Dispersion relations of the triplet (dashed lines) and singlet (full lines) collective modes of the isospin-unpolarized system of semions with Coulomb interaction for parameter values (A) $r_s=1.33$, (B) $r_s=1.89$, and (C) $r_s=2.36$.

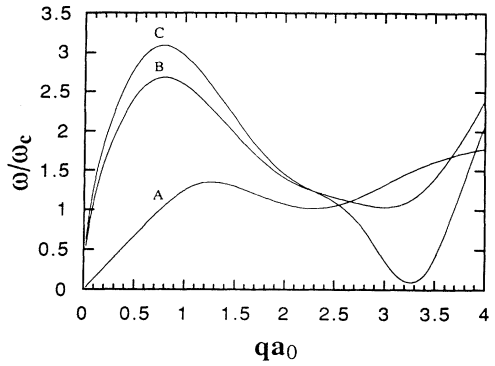

FIG. 3. Dispersion relation for the collective mode of the isospin-polarized semion system with Coulomb interaction for parameter values (*A*) $r_s=0$, (*B*) $r_s=7.35$, and (*C*) $r_s=9.95$.

We have tested the reliability of this calculation by using the same formalism to study the bose Coulomb gas. We find the instability in this system to occur at $r_s=40$, which agrees well with the Green's function Monte Carlo estimate $r_s=37\pm5$ (Ref. 17) for *fermions*.

We note that our Hartree-Fock and RPA estimates $r_s=2.53$ and 2.36 for the magnetic instabilities of the semion system are comparable in size to the Hartree-Fock result $r_s=2.2$ we find for the ferromagnetic instability of the 2D electron gas. The Hartree-Fock approximation may lead to underestimate the critical value of r_s at which magnetic instabilities occur. This is verified to be true in the case of the electron gas, for which magnetic and Wigner instabilities are found[17] to occur at comparable densities, characterized by $r_s\cong37$. In light of the analogy with the electron gas, our result $r_s\cong2.3$ for the magnetic instabilities of the semion system should therefore be regarded as a lower-bound for the critical value of r_s at which the unpolarized fluid becomes unstable. Based on the same analogy, we expect our result $r_s\cong10$ for Wigner instabilities to be relevant to the unpolarized semion system and to provide an upper bound for the critical value of r_s at which the unpolarized fluid becomes unstable.

In the context of the commensurate flux state description of the t-J model, such instabilities lead to the destruction of the superfluid phase at low density. It is interesting to evaluate the doping at which these instabilities should occur in real materials. The number of holons per lattice site is given as a function of r_s by

$$\delta=\pi^{-1}\left[b_0\frac{m^*e^2}{\varepsilon\hbar^2}\right]^2 r_s^{-2}\ , \tag{51}$$

where b_0 denotes the bond length. Using $b_0\sim4$ Å and $\varepsilon\sim6$ for the case of La_2CuO_4 and approximating the holon mass by the mass of the bare electron, we obtain a doping range of 0.006–0.11 holons per lattice site. Note that this doping range includes the domain in which La_2CuO_4 loses superconductivity and exhibits a spin-glass behavior.[13] This suggests that, within the commensurate flux state description of the t-J model, the instabilities of the system of holons with Coulomb repulsion may account for the disappearance of superfluidity at small doping.[24,3]

ACKNOWLEDGMENTS

P.B. wishes to thank J. L. Levy and Q. Dai for instruction in the use of their programs as well as A. Tikofsky, A. L. Fetter, and D. Peters for helpful discussions. This work was supported primarily by the National Science Foundation under Grant No. DMR-88-16217. Additional support was provided by the NSF MRL program through the Center for Materials Research at Stanford University and by the Lawrence Livermore National Laboratory under Contract No. W-7405-Eng-48. P.B. acknowledges financial support from the Swiss National Science Foundation.

APPENDIX

The contributions $\epsilon_n^{(13)}$ defined in Eq. (44) are given by

$$\epsilon_n^{(13)}=-r_s\sqrt{\pi/2}\prod_{i=1}^{n}\frac{(i-1/2)}{i}\ . \tag{A1}$$

The contributions $\mathcal{W}^{(21)}$ and $\mathcal{W}^{(22)}$ defined in Eq. (44) are given by

$$\begin{aligned}
&\langle {}^0_m|\mathcal{W}^{(21)}|{}^0_n\rangle=\langle {}^0_m|\mathcal{W}^{(21)}|{}^n_0\rangle=r_sce^{-b}/q\ ,\\
&\langle {}^0_m|\mathcal{W}^{(21)}|{}^1_n\rangle=\langle {}^0_m|\mathcal{W}^{(21)}|{}^n_1\rangle=r_sce^{-b(b-n)/q}\ ,\\
&\langle {}^1_m|\mathcal{W}^{(21)}|{}^0_n\rangle=\langle {}^1_m|\mathcal{W}^{(21)}|{}^n_0\rangle=r_sce^{-b(b-m)/q}\ ,\\
&\langle {}^1_m|\mathcal{W}^{(21)}|{}^1_n\rangle=\langle {}^1_m|\mathcal{W}^{(21)}|{}^n_1\rangle=r_sce^{-b(b-m)(b-n)/q}
\end{aligned} \tag{A2}$$

and by

$$\langle {}^{0}_{m}|\mathcal{W}^{(22)}|{}^{0}_{n}\rangle = -\sqrt{\pi/2}r_s c e^{-b} f(m,n), \quad \langle {}^{0}_{m}|\mathcal{W}^{(22)}|{}^{n}_{0}\rangle = -\sqrt{\pi/2}r_s c e^{-b} f(0,m+n) ,$$
$$\langle {}^{0}_{m}|\mathcal{W}^{(22)}|{}^{1}_{n}\rangle = -\sqrt{\pi/2}r_s c e^{-b}[bf(m+1,n)-nf(m,n-1)] ,$$
$$\langle {}^{0}_{m}|\mathcal{W}^{(22)}|{}^{n}_{1}\rangle = -\sqrt{\pi/2}r_s c e^{-b}[bf(1,m+n)-nf(0,m+n-1)] ,$$
$$\langle {}^{1}_{m}|\mathcal{W}^{(22)}|{}^{0}_{n}\rangle = -\sqrt{\pi/2}r_s c e^{-b}[bf(m,n+1)-mf(m-1,n)] , \tag{A3}$$
$$\langle {}^{1}_{m}|\mathcal{W}^{(22)}|{}^{n}_{0}\rangle = -\sqrt{\pi/2}r_s c e^{-b}[bf(1,m+n)-mf(0,m+n-1)] ,$$
$$\langle {}^{1}_{m}|\mathcal{W}^{(22)}|{}^{1}_{n}\rangle = -\sqrt{\pi/2}r_s c e^{-b}[b^2 f(m+1,n+1)-(m+n)bf(m,n)+mnf(m-1,n-1)] ,$$
$$\langle {}^{1}_{m}|\mathcal{W}^{(22)}|{}^{n}_{1}\rangle = -\sqrt{\pi/2}r_s c e^{-b}[b^2 f(2,m+n)-(m+n)bf(1,m+n-1)+mnf(0,m+n-2)] ,$$

where $b=q^2/2$, r_s is defined as in Eq. (39), coefficients c are given by

$$c_{mm'nn'} = \left[\frac{b^{m+n-m'-n'}}{m!n!}\right]^{1/2}\left[\frac{-z_\beta}{|z_\beta|}\right]^{n-m-n'+m'} \tag{A4}$$

and where the function $f(m,n)$ is given by

$$f(m,n) = \sum_{i=0}^{\min(m,n)} \frac{b^{-i}}{i!}\frac{m!}{(m-i)!}\frac{n!}{(n-i)!}\prod_{l=1}^{m+n-2i}\left(l-\frac{1}{2}\right)\sum_{k=0}^{\infty}\frac{b^k\prod_{j=1}^{k+i}(j-1/2)}{(m+n-i+k)!k!} . \tag{A5}$$

[1] *The Physics and Mathematics of Anyons,* edited by S. S. Chern, C. W. Chu, and C. S. Ting (World Scientific, Singapore, 1991).
[2] X. C. Xie, Song He, and S. Das Sarma, Phys. Rev. Lett. **65**, 649 (1990).
[3] R. B. Laughlin, Science **242**, 525 (1988).
[4] R. B. Laughlin, Phys. Rev. Lett. **60**, 2677 (1988).
[5] C. B. Hanna and R. B. Laughlin, Phys. Rev. B **40**, 8745 (1989).
[6] A. L. Fetter, C. B. Hanna, and R. B. Laughlin, Phys. Rev. B **39**, 9679 (1989).
[7] C. B. Hanna, R. B. Laughlin, and A. L. Fetter, Phys. Rev. B **43**, 309 (1991).
[8] Q. Dai *et al.*, Phys. Rev. B **46**, 5642 (1992).
[9] L. B. Ioffe and A. I. Larkin, Phys. Rev. B **39**, 8988 (1989).
[10] Z. Zou, J. L. Levy, and R. B. Laughlin, Phys. Rev. B **45**, 993 (1992).
[11] R. B. Laughlin and Z. Zou, Phys. Rev. B **41**, 664 (1989).
[12] Z. Zou and R. B. Laughlin, Phys. Rev. B **42**, 4073 (1990).
[13] G. Shirane *et al.*, Phys. Rev. Lett. **59**, 1613 (1987); Y. Endoh *et al.*, Phys. Rev. B **37**, 7443 (1988).
[14] A. W. Overhauser, Phys. Rev. Lett. **4**, 462 (1960).
[15] D. M. Ceperley, Phys. Rev. B **18**, 3126 (1978).
[16] D. M. Ceperley and B. Alder, Phys. Rev. Lett. **45**, 566 (1980).
[17] B. Tanatar and D. M. Ceperley, Phys. Rev. B **39**, 5005 (1989).
[18] C. Kallin and B. I. Halperin, Phys. Rev. B **30**, 5655 (1984); **31**, 3635 (1985); S. M. Girvin, A. H. MacDonald, and P. M. Platzman, Phys. Rev. Lett. **54**, 581 (1985).
[19] P. W. Anderson, *Basic Notions of Condensed Matter Physics* (Addison-Wesley, Reading, MA, 1984), p. 96.
[20] X. M. Chen and A. W. Overhauser, Phys. Rev. B **42**, 10 601 (1990).
[21] A. W. Overhauser, Phys. Rev. **128**, 1437 (1962).
[22] A. W. Overhauser, Adv. Phys. **27**, 343 (1978).
[23] A. L. Fetter, Ann. Phys. (N.Y.) **81**, 367 (1973).
[24] D. Peters and B. Alder, in *Computer Simulation Studies in Condensed Matter Physics: Recent Developments,* edited by D. P. Landau and H. B. Schlüter (Springer Verlag, Berlin, 1988).